

MIT Open Access Articles

How a Single-Point Mutation in Horseradish Peroxidase Markedly Enhances Enantioselectivity

The MIT Faculty has made this article openly available. **Please share** how this access benefits you. Your story matters.

Citation: Antipov, Eugene, Art E. Cho, and Alexander M. Klivanov. "How a Single-Point Mutation in Horseradish Peroxidase Markedly Enhances Enantioselectivity." *Journal of the American Chemical Society* 131, no. 31 (August 12, 2009): 11155-11160.

As Published: <http://dx.doi.org/10.1021/ja903482u>

Publisher: American Chemical Society

Persistent URL: <http://hdl.handle.net/1721.1/82514>

Version: Author's final manuscript: final author's manuscript post peer review, without publisher's formatting or copy editing

Terms of Use: Article is made available in accordance with the publisher's policy and may be subject to US copyright law. Please refer to the publisher's site for terms of use.



Published in final edited form as:

J Am Chem Soc. 2009 August 12; 131(31): 11155–11160. doi:10.1021/ja903482u.

HOW A SINGLE-POINT MUTATION IN HORSERADISH PEROXIDASE MARKEDLY ENHANCES ENANTIOSELECTIVITY

Eugene Antipov[†], Art E. Cho[§], and Alexander M. Klibanov^{†,‡}

[†]Department of Biological Engineering, Massachusetts Institute of Technology, Cambridge, MA 02139

[‡]Department of Chemistry, Massachusetts Institute of Technology, Cambridge, MA 02139

[§]Department of Biotechnology and Bioinformatics, Korea University, Seoul, Korea

Abstract

The effect of all possible mutations at position 178 on the enantioselectivity of yeast surface-bound horseradish peroxidase (HRP) toward chiral phenols has been investigated. In contrast to their wild-type predecessor, most HRP mutants are enantioselective, with the Arg178Glu variant exhibiting the greatest, 25-fold (*S*)/(*R*) preference. Using kinetic analysis of enzymatic oxidation of various substrate analogs and molecular modeling of enzyme-substrate complexes, this enantioselectivity enhancement is attributed to changes in the transition state energy due to electrostatic repulsion between the carboxylates of the enzyme's Glu178 and the substrate's (*R*)-enantiomer.

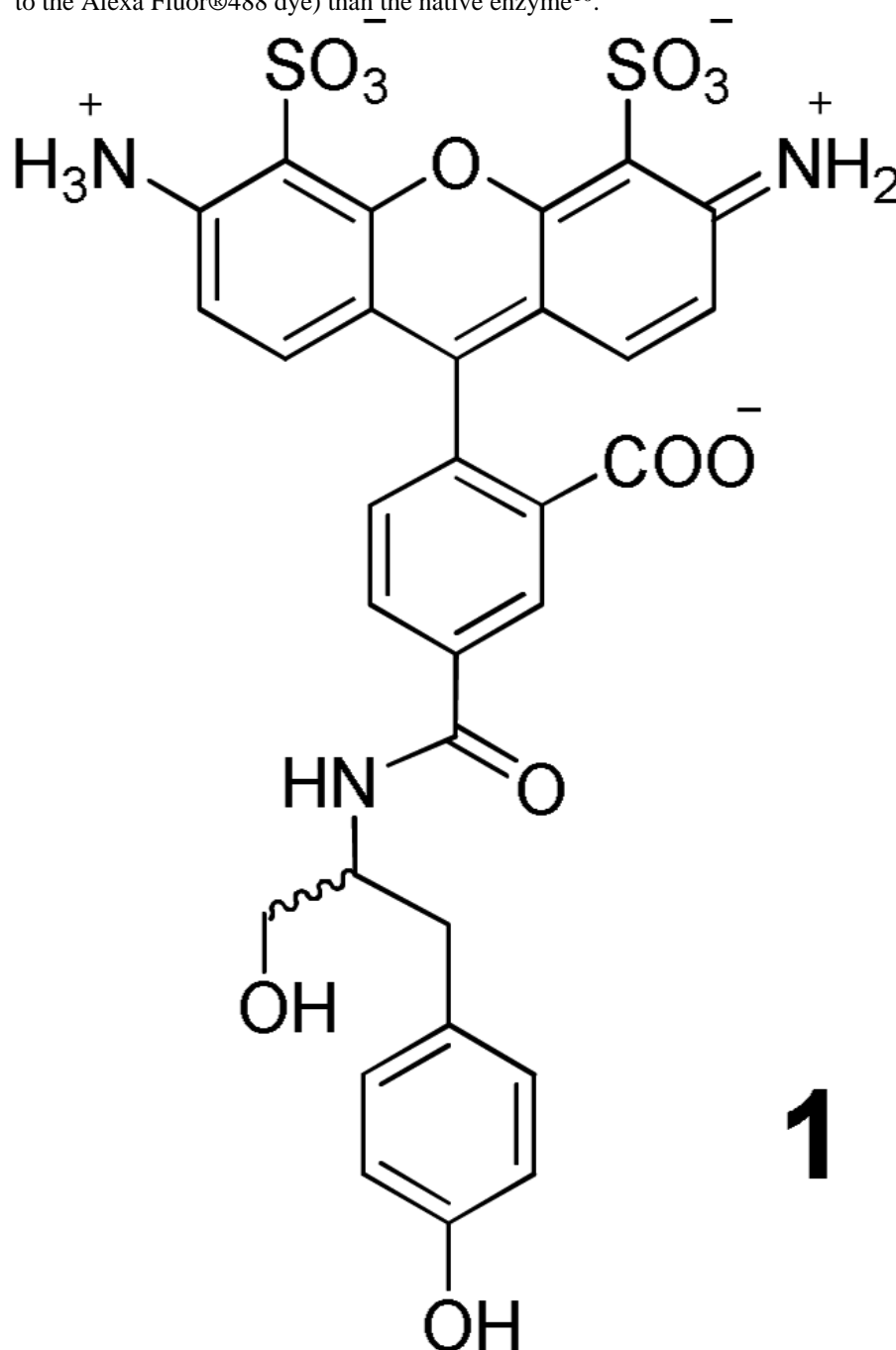
Introduction

While enzymes typically exhibit exquisite enantioselectivities toward their natural substrates, most synthetically useful substrates are non-natural¹. Therefore, there has been much effort to enhance enzymatic enantioselectivity toward these artificial substrates to create superior practical biocatalysts for organic and industrial chemistry². While the ability to rationally predict mutations that improve selectivity would be of great value, insufficient mechanistic details governing enzymatic enantioselectivity limit such approaches. Directed evolution, which requires no knowledge of enzyme structure and/or mechanism, in principle provides a promising alternative protein engineering strategy to enhance enantioselectivity³. Its success, however, depends on the efficient search of protein sequence space using high-throughput screening or selection methods, whose development remains daunting⁴. Therefore, semi-rational enzyme engineering strategies, where the search space is reduced by targeting for mutations only those residues likely to improve enzyme function, thereby resulting in smaller libraries, are emerging as powerful tools for augmenting enzymatic enantioselectivity⁵. Knowing these residues and how they exert their influence could also help the rational design of highly enantioselective enzymes⁶.

Oxidoreductases, such as horseradish peroxidase (HRP)⁷, are particularly attractive biocatalysts due to numerous asymmetric processes they catalyze⁸. Among other synthetically useful reactions, HRP catalyzes the oxidation of a variety of chiral phenols with hydrogen peroxide, albeit typically with low enantioselectivity⁹.

We recently developed an efficient directed-evolution method based on yeast surface display and fluorescence-activated cell sorting (FACS) that enabled us to dramatically improve HRP's

enantioselectivity toward certain phenols¹⁰. Using this experimental platform, we discovered an HRP variant with a single Arg-to-Gln mutation at position 178 (Arg178Gln) exhibiting an 18-fold greater enantioselectivity toward fluorescent substrate **1** (tyrosinol covalently linked to the Alexa Fluor@488 dye) than the native enzyme¹⁰.



In the present study, we elucidate mechanistically how a single mutation at position 178 of yeast surface-bound HRP leads to a marked improvement in enantioselectivity toward **1**. Moreover, using *in vitro* kinetic assays, substrate analogs, and molecular modeling, we show that a 25-fold enhancement in enantioselectivity exhibited by the Arg178Glu variant of HRP is mostly due to a change in the transition state energy stemming from the electrostatic repulsion

between the carboxylates of the (*R*)-enantiomer of the substrate and the Glu178 residue of the enzyme.

Results and Discussion

HRP is a highly glycosylated enzyme containing four disulfide bonds and a catalytically essential heme prosthetic group¹¹. Due to this structural complexity, heterologous expression of the enzyme in prokaryotes is impaired, thus necessitating a eukaryotic system to produce active HRP. Previously, we demonstrated that yeast surface display¹² was well suited for the expression, engineering, and characterization of HRP, in particular using fluorescent phenolic substrates^{10,13}. This methodology allows quantitative measurements of HRP expression and activity by flow cytometry and also enables convenient characterization of enzyme variants without soluble expression and purification of each individual clone¹⁴. Using this system, we discovered a number of HRP variants with enhanced enantioselectivities toward both the (*R*)- and (*S*)-enantiomers of **1**¹⁰. In particular, a single-point mutant isolated from a random mutagenesis library, Arg178Gln, greatly preferred the (*S*)-enantiomer, while the wild-type enzyme was virtually non-enantioselective¹⁰.

To understand the mechanism by which the single mutation at position 178 endows HRP with the keen enantioselectivity, we first investigated the relationship between the latter and the nature of the amino acid residue at this position. To this end, we mutated this residue to each of the other nineteen standard amino acids and measured the enantioselectivity of every respective surface-bound HRP variant toward the optical isomers of substrate **1**. As seen in Figure 1, the enantioselectivity, $E(S/R)$ ¹⁵, of the wild-type enzyme displayed on the cell surface of yeast was negligible — 0.8 ± 0.2 ; however, when the wild-type's Arg178 was replaced with Gln, the enantioselectivity jumped to 14 ± 1 in agreement with our previous results¹⁰.

The $E(S/R)$ values depicted in Figure 1 also show that replacing the positively charged Arg178 with the aromatic residues Tyr, Phe, or Trp produced no active enzyme variants, presumably due to steric constraints imposed by the bulky side chains¹⁶. Similarly, the Arg178Cys variant was devoid of catalytic activity, probably due to mispairing of disulfide bonds within HRP. However, all other Arg178X variants (where X is an amino acid residue) were enzymatically active, and their $E(S/R)$ analysis afforded interesting conclusions. First, preserving the positive charge at position 178 retained the enzyme's low enantioselectivity — Arg178Lys's $E(S/R) = 1.8 \pm 0.3$ — whereas all other mutations abolishing the positive charge at that position increased the $E(S/R)$ values (Figure 1). Second, reversal of the charge via the introduction of the negatively charged Asp or Glu residues sharply raised the enantioselectivity to 13 ± 1 and 20 ± 3 , respectively. Finally, the other mutants at position 178, be they hydrophobic (e.g., Val) or hydrophilic (e.g., Ser), bulky (e.g., Ile) or small (e.g., Gly), all had their $E(S/R)$ values in the same narrow intermediate range from 4 to 10. These results suggest that electrostatic interactions mediated by residue 178 are the main determinant of HRP's enantiopreference toward **1**.

To further explore the role of electrostatics, we examined the kinetics governing the highest, 25-fold improvement in enantioselectivity observed with the charge-reversed Arg178Glu variant. Since the $E(S/R)$ of HRP directly depends on the oxidation rates of both enantiomers of **1**, it can be enhanced by either increasing the oxidation rate of the (*S*)-enantiomer, or decreasing that of the (*R*)-enantiomer, or both. To determine which of these scenarios actually occurs when Arg178 is replaced with Glu, we measured the initial oxidation rates of the native and mutant enzymes with both substrate enantiomers. Table 1 shows that the wild-type enzyme, consistent with its $E(S/R)$ value being close to unity, oxidizes (*S*)-**1** and (*R*)-**1** with similar rates: 5.0 ± 0.2 and 6.3 ± 0.3 MFU/min, respectively. Interestingly, the Arg178Glu variant oxidizes (*S*)-**1** at almost the same rate as the native enzyme (6.2 ± 0.6 and 5.0 ± 0.2 MFU/min,

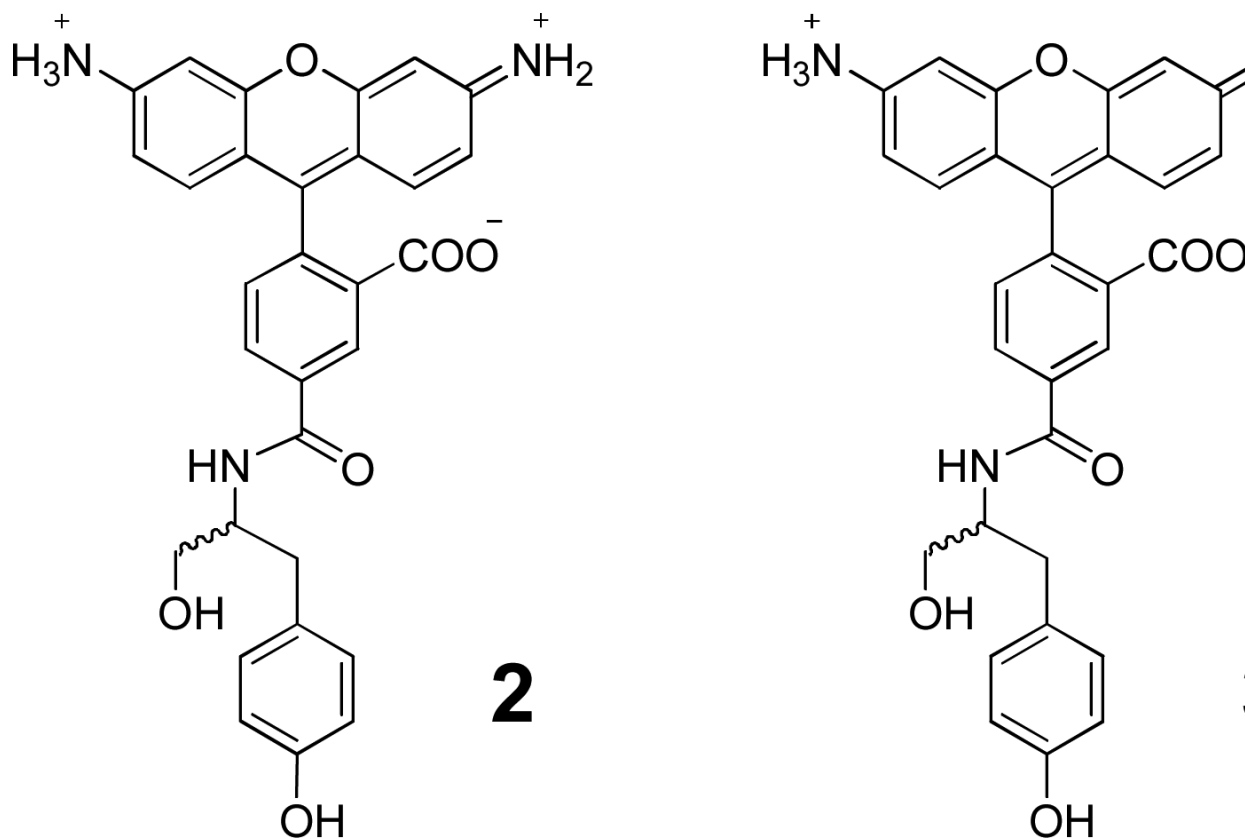
respectively), whereas the oxidation of the (*R*)-enantiomer is some 20-fold slower than that by the wild-type (0.3 ± 0.1 MFU/min and 6.3 ± 0.3 MFU/min, respectively). Thus, the 25-fold rise in enantioselectivity attained by Arg178Glu HRP is predominantly due to the plunged reactivity of (*R*)-**1**. Moreover, taken together with the mutagenesis analysis (Figure 1), these data suggest that it is largely electrostatic interactions between the (*R*)-enantiomer and the residue at position 178 in the transition state that control the enantioselectivity.

To test this hypothesis, we explored which functional groups of (*R*)-**1** are involved in this putative electrostatic interaction. Under our experimental pH (7.4), two types of anionic groups — a carboxylate and two sulfonates — may play such a role. One plausible mechanism by which Arg178Glu HRP can acquire high enantioselectivity is that the negatively charged carboxylate and/or sulfonates stabilize the transition state of the wild-type enzyme and (*R*)-**1** by forming a salt bridge with the positively charged Arg178. Replacing the latter with any amino acid residue other than Lys would eliminate this stabilizing interaction and hence lower the oxidation of the (*R*)-enantiomer. Note, however, that the oxidation rate of the (*S*)-enantiomer is similar to that of its (*R*)-counterpart for the wild-type enzyme and is almost unaffected by the Arg178Glu mutation. Therefore, the (*S*)-enantiomer must form a very different transition state with wild-type HRP than the (*R*)-enantiomer for its oxidation rate by the Arg178Glu variant to remain unaltered, while that of the (*R*)-enantiomer's is slashed some 20-fold. Another molecular mechanism also consistent with the notion that the transition states for both enantiomers with the wild-type enzyme have similar energies involves the aforementioned anionic groups of (*R*)-**1** preventing the formation of a stable activated complex between this enantiomer and the Arg178Glu variant due to an electrostatic repulsion with Glu178. To distinguish between these alternatives, we have employed molecular modeling to obtain structures of wild-type HRP complexed with each enantiomer of **1**.

As seen in Figure 2, (*S*)-**1** and (*R*)-**1** bind similarly to the wild-type enzyme with calculated binding energies of -5.41 kcal/mol and -5.89 kcal/mol, respectively. This similarity is consistent with our observation that the oxidation of (*S*)-**1** by the wild-type enzyme is just slightly slower than that of (*R*)-**1** (Table 1). Figure 2 also reveals that the sulfonate groups of both substrate enantiomers are located in proximity to Arg178: the distances between the oxygen of each sulfonate group and the closest nitrogen of the guanidinium group are 3.5 Å and 2.8 Å for the (*S*)-enantiomer and 3.1 Å and 2.8 Å for the (*R*)-enantiomer. This structural information argues against the high enantioselectivity of Arg178Glu HRP being due to the loss of a salt bridge with the sulfonates of (*R*)-**1**, since substitution of Arg178 would have led to elimination of any potential salt bridges in both the (*S*)- and (*R*)- transition states with no consequent selectivity.

These docking studies also shed light on the role of the substrate's carboxylate in mediating enantioselectivity of HRP. As seen in Figures 2A and 2C, the carboxyl group of (*S*)-**1** points away from the guanidinium group of Arg178 such that they are separated by the planar fused aromatic rings. In contrast, although the orientation of the (*R*)-**1**'s carboxyl group is conducive to making a salt bridge with this guanidinium group, a relatively large distance between them, 5.3 Å (Figure 2B), makes this scenario unlikely¹⁷. It appears, therefore, that it is the electrostatic repulsion between the carboxylate or sulfonates of (*R*)-**1** and Glu178 that plays a dominant role in imparting HRP's enantioselectivity toward **1**.

To determine which of the anionic groups of (*R*)-**1** plays the main role in this repulsion, we measured the enantioselectivity of the wild-type enzyme and the Arg178Glu variant toward **2**, a substrate analog of **1** lacking the sulfonates.



As seen in Table 1, wild-type HRP catalyzes the oxidation of **2** with a slight (*R*)-enantiopreference: $E(S/R) = 0.7 \pm 0.1$. In contrast, the Arg178Glu variant is keenly (*S*)-selective toward **2** with an $E(S/R)$ value of 13 ± 1 (Table 1), thus representing a 19-fold rise in enantioselectivity compared to the native enzyme. Therefore, the sulfonates of **1** seem insignificant in controlling the enantiopreference of Arg178Glu HRP given the similar magnitudes of the improvement in the $E(S/R)$ toward **2** and **1** (19-fold and 25-fold, respectively). This conclusion is consistent with our molecular modeling predictions that the sulfonates are close to Arg178 for both enantiomers (Figure 2) and therefore their interactions with Glu178 are unlikely to induce enantioselectivity¹⁸.

Inspection of Table 1 also reveals that while the oxidation of (*R*)-**2** by the Arg178Glu variant is some 20-fold slower than that by the wild-type enzyme (0.5 ± 0.1 and 10 ± 1 MFU/min, respectively), the oxidation rates of the (*S*)-enantiomer are similar for both enzymes. Therefore, the 19-fold increase in enantioselectivity exhibited by the Arg178Glu variant toward **2** is entirely due to a drop in the reactivity of the (*R*)-enantiomer, as is also the case with **1**. These results suggest that it is an electrostatic repulsion between the carboxylate of the substrate and the introduced glutamate residue that is responsible for the enhanced enantiopreference of Arg178Glu HRP as compared to its wild-type predecessor.

To probe these interactions further, we proceeded to model complexes of wild-type HRP with (*S*)- and (*R*)-**2**. The binding modes thus obtained (Figures 3A and 3B) resemble the ones observed with (*S*)- and (*R*)-**1** and also indicate that the carboxyl groups of the two enantiomers are oriented differently vis-à-vis Arg178. Specifically, a planar aromatic ring system of (*S*)-**2** prevents its carboxylate from interacting with Arg178 (Figure 3A). In contrast, the carboxyl group of (*R*)-**2** is positioned to directly interact with Arg178 (Figure 3B); in this orientation it is also likely to experience an electrostatic repulsion with Glu178 which, in turn, would weaken

the binding of (*R*)-**2** in the transition state, thereby making the Arg178Glu variant highly (*S*)-selective, as is actually observed.

To ascertain whether this electrostatic repulsion is indeed important in determining the enantioselectivity toward **2**, we measured the initial oxidation rates of both substrate enantiomers with the wild-type and Arg178Glu enzymes in the presence of a high salt concentration. As seen in Table 2, both enzymes are more active at 1 M NaCl than at 137 mM NaCl¹⁹. The enantioselectivity of wild-type HRP in these high-salt and low-salt buffered solutions were the same (0.9 ± 0.2 and 0.7 ± 0.1 , respectively), indicating that the putative electrostatic attraction between the carboxylate of (*R*)-**2** and Arg178 is insensitive to the salt concentration²⁰. In contrast, the enantioselectivity of the Arg178Glu variant was nearly 3-fold lower in the high-salt than in the low-salt solution: the $E(S/R)$ values were 4.9 ± 0.6 and 13 ± 1 , respectively. Furthermore, Table 2 shows that this drop in the $E(S/R)$ stems from an increase in the oxidation rate of the (*R*)-enantiomer consistent with the proposed electrostatic repulsion between the carboxylates of (*R*)-**2** and Glu178, which expectedly was partially alleviated by the presence of high salt.

We thus reasoned that eliminating this repulsion by neutralizing the negative charge of the substrate's carboxylate should increase the oxidation rate of the (*R*)-enantiomer and hence restore the wild-type-like level of HRP's enantioselectivity. Computational docking of methyl esters of (*R*)-**2** and (*S*)-**2** (i.e., (*R*)-**3** and (*S*)-**3**, respectively) to the wild-type enzyme yielded binding modes similar to those observed with their respective carboxylate counterparts, suggesting that the esterification would only affect the proposed electrostatic repulsion (Figure 3).

To test these computer-modeling-based predictions, we synthesized (*S*)-**3** and (*R*)-**3** and measured their initial oxidation rates catalyzed by the wild-type enzyme and the Arg178Glu variant (rows 3 and 4 in Table 1). As predicted, wild-type HRP exhibited similar enantioselectivities with **2** and **3**: $E(S/R)$ were 0.7 ± 0.1 and 1.1 ± 0.1 , respectively. Importantly, protecting the carboxyl group (in substrate **3** compared to **2**) indeed restored the oxidation rate of the (*R*)-enantiomer by the Arg178Glu variant to that of the wild-type enzyme (8.9 ± 0.3 and 8.4 ± 0.2 MFU/min, respectively; Table 1). This significant rise in the oxidation rate of (*R*)-**3** by Arg178Glu HRP points to the electrostatic repulsion between the carboxylates of the (*R*)-enantiomer of **1** or **2** and Glu178 in the transition state as the defining mechanism of the enhanced enantioselectivity of this enzyme variant²¹.

In summary, we have found herein that while eliminating the positive charge in the side chain of residue 178 moderately increases the enantioselectivity of yeast surface-bound HRP toward **1**, replacing it with a negatively charged one induces a far greater effect. Aided by structure-based molecular modeling, we have rationalized that a 25-fold enhancement in enantioselectivity for the charge-reversed Arg178Glu HRP is primarily caused by a slower oxidation rate of the (*R*)-enantiomer which, in turn, is due to the electrostatic repulsion between the carboxyl groups of this enantiomer and Glu178 of the enzyme in the transition state. Overall, our analysis suggests that molecular modeling in combination with *in vitro* kinetic assays and substrate analog studies provide useful mechanistic insights into enzyme enantioselectivity and how to improve it.

Materials and Methods

Materials

All chemicals were purchased from Sigma-Aldrich Chemical Co. (St. Louis, MO) unless stated otherwise and were of the highest purity available from the vendor. The enantiomers of substrate **1** were synthesized as previously described¹⁰. The enantiomers of substrate **2** were

prepared by reacting L- or D- [(S) or (R), respectively] tyrosinol with 5-carboxyrhodamine 110 succinimidyl ester (AnaSpec, San Jose, CA) according to the following procedure²². The fluorescent dye (2 mg, 4 μ mol) was added to a solution of L- or D-tyrosinol (2.4 mg, 12 μ mol) and triethylamine (24 μ mol) in DMF (1 mL). The resulting mixture was stirred at room temperature for 3 h, evaporated, and re-dissolved in 10% (v/v) acetonitrile/water (1 mL). The product was purified by reverse-phase HPLC using a 9.4 \times 250 mm 5 μ M SB-Phenyl column (Agilent Technologies, Santa Clara, CA) with 100 mM triethylammonium acetate buffer (pH 7.0) (Calbiochem, San Diego, CA) as a loading buffer and acetonitrile as a mobile phase. The product was eluted with a 30-min, 4 mL/min gradient of 10%-100% acetonitrile. The enantiomers of substrate **3** were prepared by dissolving those of dry crude substrate **2** product in 1% H₂SO₄ (v/v) in anhydrous methanol (3 mL). The mixture was refluxed for 2 days, evaporated, and neutralized to pH 7 by saturated aqueous NaHCO₃. The product was purified by reverse-phase HPLC under the same conditions as used to purify **2**. The identity of all the substrates was confirmed by electrospray ionization (ESI)-MS.

Mutations at position 178 of HRP were made using the QuikChange site-directed mutagenesis kit (Stratagene, La Jolla, CA). HRP variants were displayed on the cell surface of the *Saccharomyces cerevisiae* yeast according to the published procedure^{10,13}. Briefly, the HRP-containing plasmids were transformed into the yeast surface display strain of *S. cerevisiae*, EBY100, using the Frozen-EZ Yeast Transformation II kit (Zymo Research, Orange, CA). The resultant colonies were grown to an OD₆₀₀ of 5–7 in 5 mL of synthetic defined (SD) medium (2% dextrose, 0.34% yeast nitrogen base without (NH₄)₂SO₄, 0.8% casamino acids (VWR, West Chester, PA), and 50 mM Na phosphate buffer adjusted to pH 6.6) by shaking at 250 rpm at 30 °C. To induce expression of HRP, the cells were centrifuged to remove the supernatant and resuspended in 5 mL of the SD medium where dextrose was replaced with galactose and supplemented with 50 μ g/mL kanamycin, 100 U/mL penicillin G, 200 U/mL streptomycin, 0.034%, thiamine HCl, 0.084% δ -aminolevulinic acid, and 0.1 mM ferric citrate. The cultures were shaken at 250 rpm at 30 °C for 19–21 h. The induced cells were then washed with phosphate-buffered saline (PBS) containing 0.5% BSA, followed by another wash with PBS alone, and used directly in the enzymatic reactions.

Enzymatic reactions

The initial oxidation rates catalyzed by surface-bound HRP were determined by suspending 1×10^6 HRP-displaying yeast cells in 100 μ L of PBS solution (pH 7.4, 137 mM or 1 M NaCl) containing 15 μ M fluorescent substrate and 150 μ M H₂O₂ in parallel for both enantiomers. Three data points for each sample were collected by periodically withdrawing 30 μ L of the *S* and *R* substrate mixtures into 1 mL of PBS containing 0.5% BSA and 10 mM ascorbic acid to quench the reactions. The fluorescently labeled yeast cells from each data point were then analyzed using a Coulter Epics XL flow cytometer (Fullerton, CA). The mean fluorescence of 30,000 cells was plotted as a function of time to determine the initial reaction rates. Enantioselectivity, $E(S/R)$, was calculated as the ratio of the initial rate of the enzymatic oxidation of the (*S*)-enantiomer divided by that of the (*R*)-enantiomer²³.

The initial reaction rates for the wild-type and Arg178Glu HRP were determined by monitoring the enzymatic reaction above except that mean fluorescence of each data point was acquired from analyzing HRP-displaying cells with the same enzyme surface concentration, which were identified using fluorescently labeled antibodies against the c-Myc epitope tag fused to HRP. To this end, the cells from each data point of enzymatic reaction were washed with 0.5 mL of PBS with 0.1% BSA and labeled with mouse anti-Myc monoclonal 9E10 (Covance, Princeton, NJ) and phycoerythrin-goat anti-mouse antibodies, as described previously^{10,13}, and analyzed using a Coulter Epics XL flow cytometer. The mean fluorescence of 30,000 cells

with the same surface concentration of HRP was then plotted as a function of time to determine the initial reaction rates.

Computational modeling

Molecular models of HRP-substrate complexes were built on the basis of the published X-ray crystal structure of HRP and its complex with ferulic acid²⁴, which was obtained by retrieving the heavy atom coordinates (entry 7ATJ) from the Brookhaven Protein Data Bank. The complexes of HRP with the substrates described in this study were generated by using a docking method that integrates quantum mechanical calculations with Schrödinger Glide version 4.5. Protein preparation wizard of Schrödinger software was used to prepare the original PDB file for docking and further modeling. With heavy atoms fixed, hydrogen atoms were added and their positions were optimized using the IMPACT²⁵ molecular minimization tool. The substrates were geometry-optimized first in molecular mechanics with MacroModel using the OPLS2005 force field and then in quantum mechanics using the Poisson-Boltzmann implicit solvent model of aqueous environment simulation. Quantum mechanics were represented by density functional theory with B3LYP functional²⁶ and 6-31G* basis set²⁷.

Current docking methods generally employ force-field-based energy scoring with various search algorithms^{28,29}. This approach, however, is inadequate to model enzymes that contain metal ions in the active site^{30,31}. The presence of iron in the HRP's heme group requires the use of quantum chemical calculations of the complex region that involves electron transfer in order to correctly predict binding modes. Therefore, a modified version of the previously described QM/MM (quantum mechanics/molecular mechanics) docking algorithm³² was used according to the following procedure. A total of 10 diverse poses were generated for each substrate: 5 poses were generated with Schrödinger Glide version 4.5 and 5 more poses were generated using “restricted docking”, wherein the phenol ring of ferulic acid in the complex with wild-type HRP served as the restriction point within prescribed tolerance (2 Å of RMSD for the carbon atoms of the phenol ring of the substrate). In order to accurately score these poses, QM/MM single-point energy calculations without geometry optimization were carried out, treating the heme group and the substrate as a quantum region. Upon convergence of these calculations, the atomic charges were fitted for atoms in the quantum region using the ESP (electrostatic potential) method. Binding energy calculations using Glide's score-in-place function were then performed to identify the lowest binding energy pose.

Acknowledgement

This work was financially supported by grant R01-GM66712 from the U.S. National Institutes of Health. We are grateful to Prof. K. Dane Wittup (Massachusetts Institute of Technology) for allowing us to use his flow cytometer. We thank Keith Miller for help in making some of the HRP mutants and Dr. Stephen Sazinsky for helpful discussion.

Footnotes and References

1. a Schoemaker HE, Mink D, Wubbolts MG. Science 2003;299:1694. [PubMed: 12637735] b Panke S, Wubbolts M. Curr. Opin. Chem. Biol 2005;9:188. [PubMed: 15811804]
2. a Klibanov AM. Nature 2001;374:596. [PubMed: 7715696] b Turner NJ. Curr. Opin. Biotechnol 2003;14:401. [PubMed: 12943849] c Reetz MT. Proc. Natl. Acad. Sci. U.S.A 2004;101:5716. [PubMed: 15079053]
3. Arnold FH. Nature 2001;409:253. [PubMed: 11196654]
4. a Tao HY, Cornish VW. Curr. Opin. Chem. Biol 2002;6:858. [PubMed: 12470742] b Reetz MT. Adv. Catal 2006;49:1.
5. a Lutz S, Patrick WM. Curr. Opin. Biotechnol 2004;15:291. [PubMed: 15296927] b Chaparro-Riggers JF, Polizzi KM, Bommarius AS. Biotechnol. J 2007;2:180. [PubMed: 17183506] c Fox RJ, Davis SC, Mundorff EC, Newman LM, Gavrilovic V, Ma SK, Chung LM, Ching C, Tam S, Muley S, Grate J,

- Gruber J, Whitman JC, Sheldon RA, Huisman GW. *Nat. Biotechnol* 2007;25:338. [PubMed: 17322872]
6. a Rotticci D, Rotticci-Mulder JC, Denman S, Norin T, Hult K. *ChemBioChem* 2001;2:766. [PubMed: 11948859] b Park S, Morley KL, Horsman GP, Holmquist M, Hult K, Kazlauskas RJ. *Chem. Biol* 2005;12:45. [PubMed: 15664514] c Ijima Y, Matoishi K, Terao Y, Doi N, Yanagawa H, Ohta H. *Chem. Commun* 2005:877. d Ema T, Fujii T, Ozaki M, Korenaga T, Sakai T. *Chem. Commun* 2005:4650. e Reetz MT, Puls M, Carballera JD, Vogel A, Jaeger KE, Eggert T, Thiel W, Bocola M, Otte N. *ChemBioChem* 2007;8:106. [PubMed: 17133645]
7. a Ling K, Li W, Sayre LM. *J. Am. Chem. Soc* 2008;130:933. [PubMed: 18163622] b Gorris H, Walt D. *J. Am. Chem. Soc* 2009;131:6277. [PubMed: 19338338]
8. a Azevedo AM, Martins VC, Prazers DM, Vojinovic V, Cabral JM, Fonseca LP. *Biotechnol. Annu. Rev* 2003;9:199. [PubMed: 14650928] b van Deurzen MPJ, van Rantwijk F, Sheldon RA. *Tetrahedron* 1997;53:13183.
9. Gilabert MA, Fenoll LG, Garcia-Molina F, Garcia-Ruiz PA, Tudela J, Garcia-Canovas F, Rodriguez-Lopez JN. *J. Biol. Chem* 2004;385:1177.
10. Antipov E, Cho AE, Wittrup KD, Klivanov AM. *Proc. Natl. Acad. Sci. U.S.A* 2008;105:17694. [PubMed: 19004779]
11. a Veitch NC. *Phytochemistry* 2004;65:249. [PubMed: 14751298] b Ryan BJ, Carolan N, O'Fagain C. *Trends Biotechnol* 2006;24:355. [PubMed: 16815578]
12. Gai SA, Wittrup KD. *Curr. Opin. Struct. Biol* 2007;17:467. [PubMed: 17870469]
13. Lipovšek D, Antipov E, Armstrong KA, Olsen MJ, Klivanov AM, Tidor B, Wittrup KD. *Chem. Biol* 2007;14:1176. [PubMed: 17961829]
14. Oxidation of fluorescent phenolic substrates by surface-bound HRP produces phenolic radicals that are captured by the cell surface, thereby fluorescently labeling the yeast cells. Fluorescence intensity of these cells, measured by flow cytometry, is directly proportional to the catalytic activity of the enzyme. An epitope tag fused to HRP allows quantitative determination of the enzyme concentration using fluorescently labeled antibodies
15. Defined as the ratio of the initial rate of the enzymatic oxidation of the (*S*)-enantiomer divided to that of the (*R*)-enantiomer
16. This supposition is supported by computational docking of these HRP variants with **1** which indicates that the substitution of Arg178 with bulky aromatic residues makes the active site inaccessible to **1** (data not shown). We are unable to measure catalytic activity of these variants using smaller phenols, as our methodology does not allow characterization of the surface-bound enzyme using non-fluorescent substrates
17. The increased enantioselectivity of HRP variants with amino acids substitutions that remove the positive charge at position 178 may be explained by the presence of a putative cation- π interaction between Arg178 (or Lys178) and Phe179. Elimination of this interaction shifts the position of Phe179 — a residue shown to be critical in substrate binding (Veitch NC, Gao Y, Smith AT, White CG. *Biochemistry* 1997;36:14751. [PubMed: 9398195]) — thereby sterically hindering binding of **1** and, in turn, influencing the enantioselectivity of these variants
18. It is also possible, however, that the sulfonates are not involved because they form intramolecular salt bridges with the neighboring protonated amino groups
19. Altering the strength of electrostatic interactions by varying salt concentration in solution is commonly used in enzyme studies (Honig B, Nicholls A. *Science* 1995;268:1144. [PubMed: 7761829])
20. In contrast to such conventional electrostatic interactions as salt bridges, cation- π interactions have been shown to be essentially insensitive to salt concentration in solution (Berry BW, Elvekrog MM, Tommos C. *J. Am. Chem. Soc* 2007;129:5308. [PubMed: 17417844])
21. It should be noted that the enantioselectivity of the Arg178Glu enzyme toward **3** differs from that of the wild-type enzyme (2.4 ± 0.1 vs. 1.1 ± 0.1 , respectively) caused by a surprising doubling in the oxidation rate of the (*S*)-enantiomer (Table 1)
22. Takakusa H, Kikuchi K, Urano Y, Kojima H, Nagano T. *Chem. Eur. J* 2003;9:1479.
23. Note that when we doubled the concentrations of (*S*)- and (*R*)- **1** to 30 μ M, the initial rates of their enzymatic peroxidation also doubled. Therefore, the K_m values must far exceed this concentration

range, i.e., the wild-type enzyme is far from being saturated with either enantiomer of **1**; in other words, the $k_{\text{cat}}/K_{\text{M}}$ regime is at play

24. Henriksen A, Smith AT, Gajhede M. J. Biol. Chem 1999;274:35005. [PubMed: 10574977]
25. Banks JL, et al. J. Comput. Chem 2005;26:1752. [PubMed: 16211539]
26. Becke AD. J. Chem. Phys 1993;98:1372.
27. Rassolov VA, Pople JA, Ratner MA, Windus TL. J. Chem. Phys 1998;109:1123.
28. Abagyan R, Totrov M. Curr. Opin. Chem. Biol 2001;5:375. [PubMed: 11470599]
29. Halperin I, Ma B, Wolfson H, Nussinov R. Proteins 2002;47:409. [PubMed: 12001221]
30. Cho AE. BioChip J 2007;1:70.
31. Cho AE. BioChip J 2008;2:148.
32. Cho AE, Rinaldo D. J. Comput. Chem. 2009DOI: 10.1002/jcc.21270
33. Boder ET, Witttrup KD. Nat. Biotechnol 1997;15:553. [PubMed: 9181578]

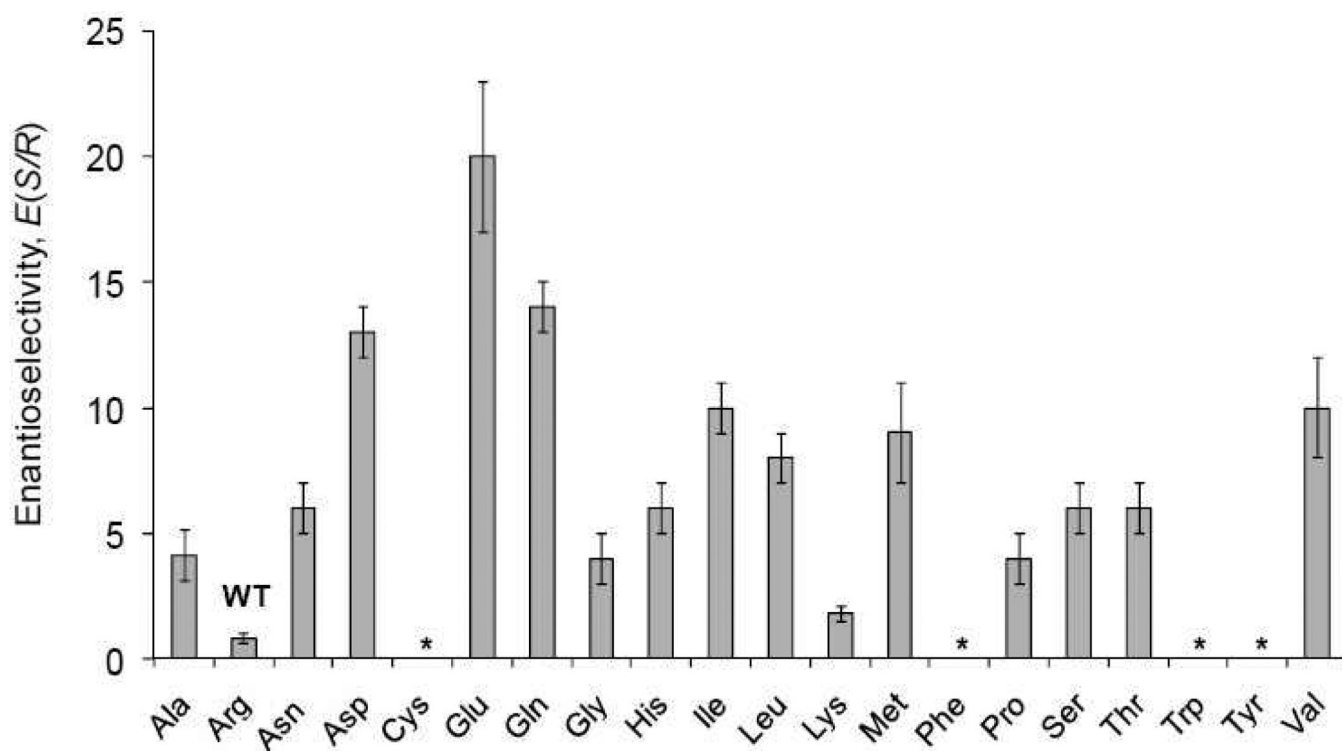


Figure 1.

Enantioselectivities¹⁵ of yeast surface-bound wild-type HRP and its 19 amino acid variants at position 178 toward a fluorescent phenolic substrate (**1**). Oxidation of **1** by surface-bound HRP yields fluorescently labeled cells whose fluorescence intensity is a direct estimate of the product amount of the enzymatic reaction. The reaction rates are defined as temporal changes in the fluorescent intensity of HRP-displaying yeast cells measured by flow cytometry. Asterisks designate catalytically inactive variants.

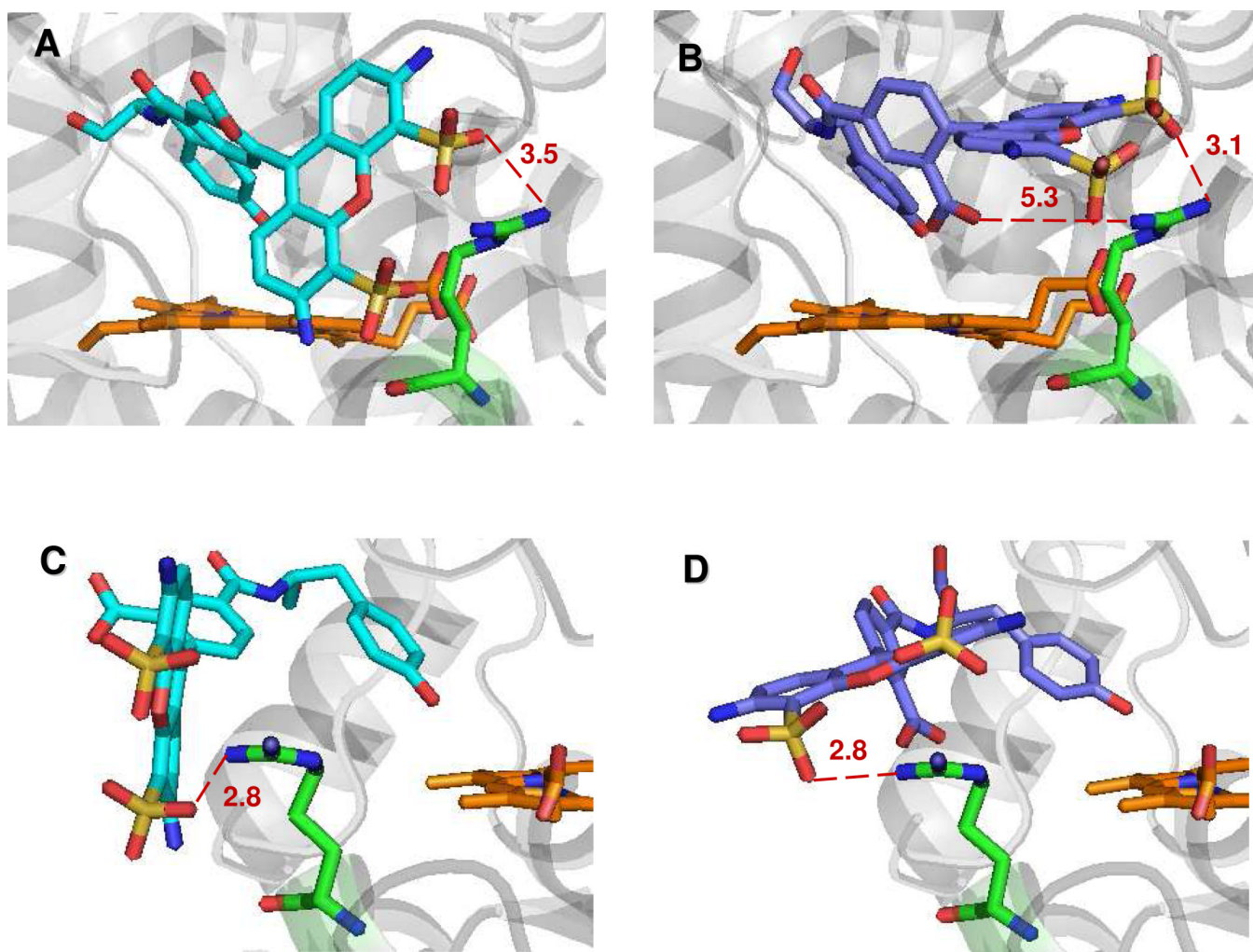


Figure 2.

Modeled complexes of wild-type HRP with (*S*)-**1** (A, C) and (*R*)-**1** (B, D). (A) and (B) show the front view of the active site; (C) and (D), respectively, show the active site rotated 90° clockwise along the z-axis. For clarity, HRP's backbone is shown in ribbon with the heme moiety in orange, substrate in blue, and Arg178 in green ball-and-stick. Distances shown are in Å. See *Methods* for details of how these molecular models were built.

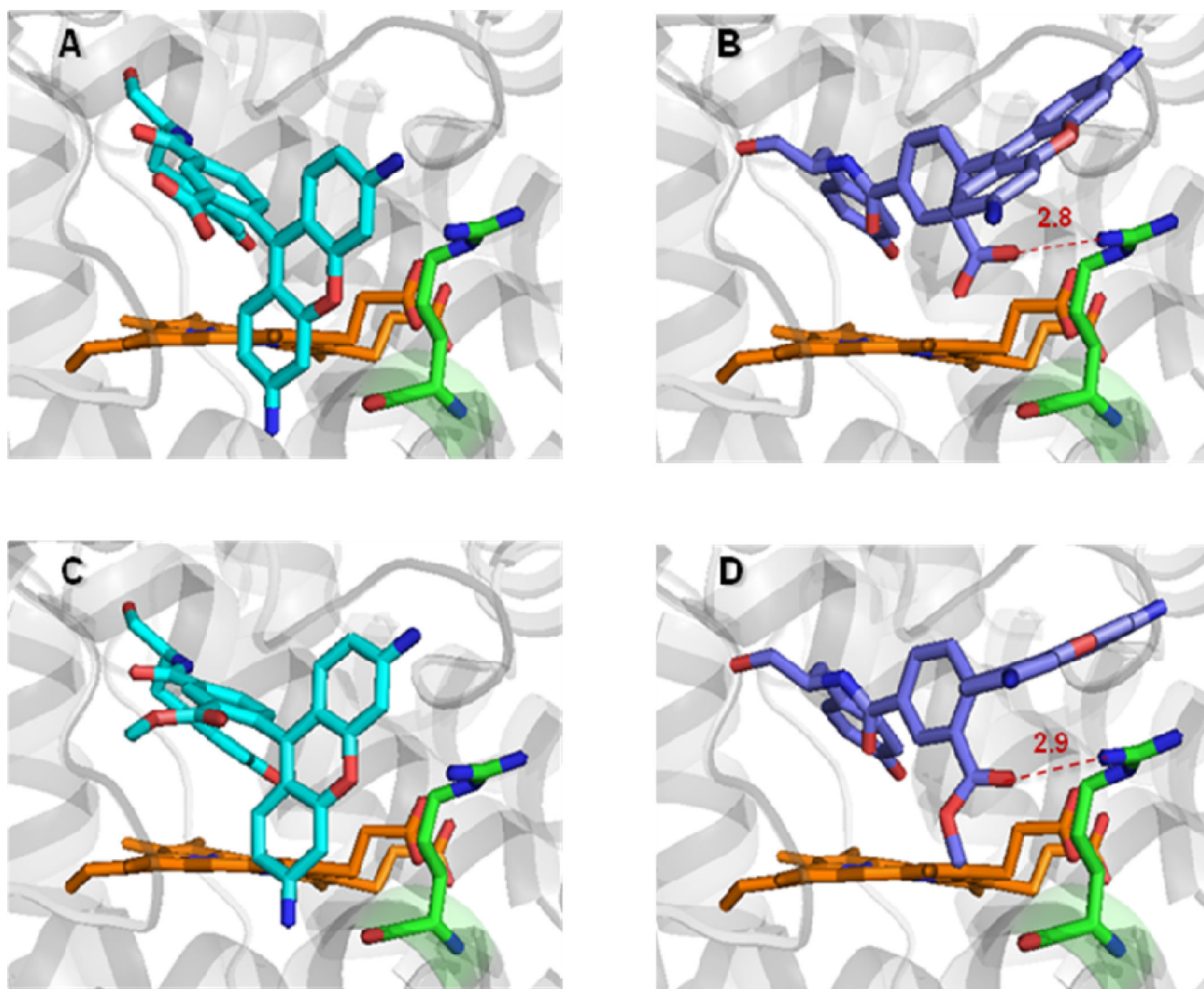


Figure 3. Modeled complexes of wild-type HRP with (*S*)-**2** (A), (*R*)-**2** (B), (*S*)-**3** (C), and (*R*)-**3** (D). For clarity, HRP's backbone is shown in ribbon with the heme moiety in orange, substrate in blue, and Arg178 in green ball-and-stick. Distances shown are in Å. See *Methods* for details of how these molecular models were built.

Table 1Initial rates and enantioselectivities of oxidation of **1**, **2**, and **3** by yeast surface-bound wild-type and Arg178Glu HRP.

HRP variant	Substrate	V_S , MFU/min ^a	V_R , MFU/min ^a	$E(S/R)$ ¹⁵
Wild-type	1	5.0 ± 0.2	6.3 ± 0.3	0.8 ± 0.2
Arg178Glu	1	6.2 ± 0.6	0.3 ± 0.1	20 ± 3
Wild-type	2	7.3 ± 0.2	10 ± 1	0.7 ± 0.1
Arg178Glu	2	6.4 ± 0.2	0.5 ± 0.1	13 ± 1
Wild-type	3	9.2 ± 0.5	8.4 ± 0.2	1.1 ± 0.1
Arg178Glu	3	21 ± 1	8.9 ± 0.3	2.4 ± 0.1

^a V_S and V_R are the initial rates of oxidation of the (S)- and (R)- enantiomer, respectively, reported in Mean Fluorescence Units (MFU) per min. MFUs represent mean fluorescence intensity of 3×10^4 HRP-displaying yeast cells that captured fluorescent products during the time of the enzymatic reaction. Each yeast cell displays approximately 3×10^4 HRP molecules on its surface³³. The initial rates are not absolute as fluorescence intensity varies for each substrate; however, their ratios giving the $E(S/R)$ values are unaffected by these variations. All experiments were conducted at least in triplicate with the mean and standard deviation values given in the table. See *Methods* for experimental details.

Table 2

The effect of salt (NaCl) concentration on enantioselectivity of yeast surface-bound wild-type and Arg178Glu HRP toward **2**.

HRP variant	Substrate	$V_S^{\text{high}} / V_S^{\text{low}}$ ^a	$V_R^{\text{high}} / V_R^{\text{low}}$ ^b	$E(S/R)$ ^c
Wild-type	2	2.1 ± 0.1	1.7 ± 0.2	0.9 ± 0.2
Arg178Glu	2	2.0 ± 0.2	5.5 ± 0.2	4.9 ± 0.6

^a $V_S^{\text{high}} / V_S^{\text{low}}$ is the ratio of the initial rates of oxidation of the (*S*)-enantiomer measured in a phosphate buffer with final NaCl concentrations of 1 M and 137 mM, respectively. All experiments were conducted at least in triplicate with the mean and standard deviation values given in the table.

^b $V_R^{\text{high}} / V_R^{\text{low}}$ is the ratio of the initial rates of oxidation of the (*R*)-enantiomer measured in a phosphate buffer with final NaCl concentrations of 1 M and 137 mM, respectively. All experiments were conducted at least in triplicate with the mean and standard deviation values given in the table.

^c Enantioselectivity, $E(S/R)$ ¹⁵, is measured in a phosphate buffer with a final 1 M NaCl concentration.